International Journal of Innovative Computing, Information and Control
Volume **22**, Number **1**, February **2026**

ICIC International ©2026 ISSN 1349-4198
pp. **301–318**

OPTIMAL COST DESIGN FOR STRIP FOOTINGS ASSUMING THAT THE GROUND CONTACT AREA IS PARTIALLY COMPRESSED

Rosa Margarita Luévanos-Soto[1], Arnulfo Luévanos-Rojas[1,*] and Inocencio Luévanos-Soto[2]

[1]Instituto de Investigaciones Multidisciplinaria
Facultad de Contaduría y Administración
Universidad Autónoma de Coahuila, Unidad Torreón
Blvd. Revolución 151 Ote. CP 27000, Torreón, Coahuila, México
r_luevanos@uadec.edu.mx; *Corresponding author: arnulfoluevanos@uadec.edu.mx

[2]Facultad de Ingeniería, Ciencias y Arquitectura
Universidad Juárez del Estado de Durango, Unidad Gómez Palacio
Av. Universidad S/N, Fracc. Filadelfia, CP 35010, Gómez Palacio, Durango, México
inocencio.luevanos@ujed.mx

Received August 2025; revised December 2025

Abstract. *This paper presents a new model to determine the minimum design cost of a strip footing to obtain the longitudinal and transverse steel area, the thickness, assuming that the soil is elastic, the distribution of soil pressures is linear and the surface in contact with the soil is partially compressed. The equations for determining the minimum area in plan are previously described by the same authors in a complementary article. Some studies consider a constant soil pressure beneath the foundation because the wall is located at the center of the base, but they do not take account of the property lines that may appear in many cases (Area works entirely under compression). The formulation is shown by integration to investigate moments and shear forces at critical sections according to the ACI code (Area is partially compressed). Four numerical studies are presented to obtain the minimum design cost of strip footings subjected to a uniformly distributed load on all walls. The results show that the new model is more economical than the current model except when the pressure generated by the soil on the footing is uniform, and the greatest savings occur at 98.89% compared to the current model; therefore, it is recommended to use the new model to solve boundary problems.*
Keywords: Optimal cost design, Stripfootings, Linear soil pressure distribution, Contact area partially compressed

1. **Introduction.** A strip footing is a type of shallow foundation used to collect and distribute the loads of three or more pillars. This structure transfers loads to the ground through load-bearing walls constructed of concrete, brick, block, stone, or other materials. Strip footing foundations offer significant structural advantages, but their optimal performance depends on proper construction.

The choice of the type of strip footing to implement depends on the loads it must support and the structural characteristics of the project. In the construction field, two main types of strip footings are recognized.

1) The central strip footing is placed directly beneath the main load-bearing walls, optimizing load distribution to the ground. Its symmetrical design with respect to the

DOI: 10.24507/ijicic.22.01.301

wall axis allows for efficient and uniform stress transmission, significantly reducing the risk of landslides or differential settlement.

2) The boundary strip footing is a perimeter foundation designed to support the loads of walls and pillars located near property boundaries. This type of footing allows for adequate load distribution, especially when the loads are eccentric, that is, when they do not rest on the centroid of the structure.

Figure 1 shows the distribution of soil pressure under a foundation according to the soil type and the foundation stiffness. Figure 1(a) presents a rigid foundation on sandy. Figure 1(b) shows a rigid foundation on clay. Figure 1(c) presents a flexible foundation on sandy. Figure 1(d) shows a flexible foundation on clay. Figure 1(e) presents a uniform distribution used in the current design [1].

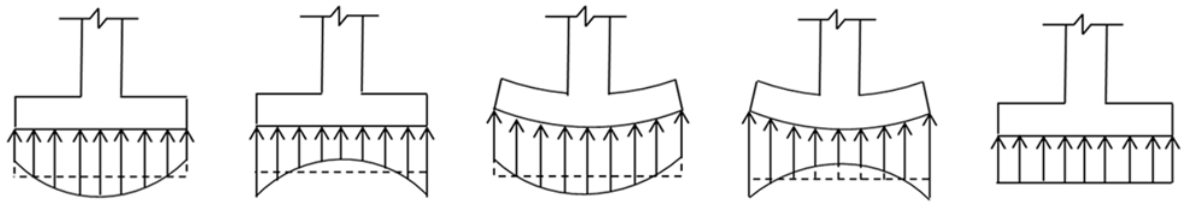

FIGURE 1. Distribution of the soil pressure under foundation

The main studies on isolated footings, combined footings and foundation slabs have been analyzed in the previous work proposed by Luévanos-Soto et al. [2], where the articles cited to determine the minimum area under the footing are shown in [3-18] and to obtain the minimum cost for the complete design are shown in [19-31]. All these articles assumed that the contact area beneath the foundation soil is working entirely under compression. Articles are also cited where it is assumed that the area in contact with the soil is partially working in compression for rectangular, square and circular isolated footings [32-44] and for rectangular combined footings [45] to determine the minimum area under the footing, and for the complete design of rectangular, square and circular isolated footings [46-48]. Other articles cited in this work determine the load capacity of strip footings under different types of loads [49-58].

According to the literature review, several studies address the bearing capacity and settlement of strip footings supported on ground [49-58], and other works present complete designs for rectangular, square, and circular isolated footings (area in contact with the ground partially compressed) [46-48]. Therefore, no work exists on the minimum design cost for strip footings assuming that the area in contact with the ground is partially in compression.

This article describes a model to determine the minimum design cost for strip footings assuming that the area in contact with the ground is partially in compression to determine the longitudinal and transverse steel area and the thickness, and this model is based on data such as $A_{\min}$ (minimum area), L_e (length of outer wall), L_i (length of inside wall), w_e (width of the outer foundation), w_i (width of the inside foundation), b (width of outer wall), y_e (distance from the center of the base to the outer edge of the base) presented by Luévanos-Soto et al. [2]. Some studies consider a constant soil pressure beneath the foundation because the wall is located at the center of the base, but they do not take account of the property lines that may appear in many cases (Area works entirely under compression). Four numerical studies are presented to determine the minimum design cost of strip footings subjected to a uniformly distributed load on all walls. A comparison is

made between the current model and the new model to verify the advantages of the new model over the current model.

The paper is organized as follows. Section 2 presents the formulation of the model to obtain the minimum design cost of a strip footing (current model and new model) assuming that contact surface with the ground is partially compressed. Subsection 2.1 describes the equations for case I or current model (Area works entirely in compression). Subsection 2.2 shows the equations for case II or new model (Area works partially in compression and the neutral axis falls within the flanges). Subsection 2.3 describes the equations for case III or new model (Area works partially in compression and the neutral axis falls within the web). Subsection 2.4 presents the equations for the minimum design cost of a strip footing. Section 3 shows the numerical studies applied to the three models for a strip footing. Section 4 presents the results. Section 5 shows the conclusions to complete the paper.

2. Formulation of the Model.

This work is formulated under the assumption: the foundation is totally rigid and rests on an elastic and homogeneous soil, that is, the soil pressure under the foundation behaves linearly according to Bowles [1], and McCormac and Brown [59].

The ultimate or factored soil pressure "p_{us}" at any point at the base of a foundation is determined from Equation (1) of Luévanos-Soto et al. [2]:

$$p_{us} = \frac{P_u}{A} + \frac{M_{ux}y}{I_x} + \frac{M_{uy}x}{I_y} \tag{1}$$

where P_u is the ultimate axial load in kN, M_{ux} is the ultimate moment on the X axis in kN-m, M_{uy} is the ultimate moment on the Y axis in kN-m, x and y are the coordinates of the pressure point under study in m, A is the area of the footing seen in plan in m^2, and I_x and I_y are the moments of inertia on the X and Y axes in m^4. $P_u = 1.2P_D$ (dead load) + $1.6P_L$ (live load), $M_{ux} = 1.2M_{Dx}$ (dead load moment) + $1.6M_{Lx}$ (live load moment), $M_{uy} = 1.2M_{Dy}$ (dead load moment) + $1.6M_{Ly}$ (live load moment) [60].

When the strip footings are not limited, the first part of Equation (1) is used for design, i.e., only P_u/A. Now, to solve the problem of border walls along property lines, transverse walls to the border wall are proposed to prevent overturning.

Figure 2 represents a strip footing that supports two types of walls. Figure 2(a) indicates a footing supporting masonry walls. Figure 2(b) indicates a footing that supports reinforced concrete walls.

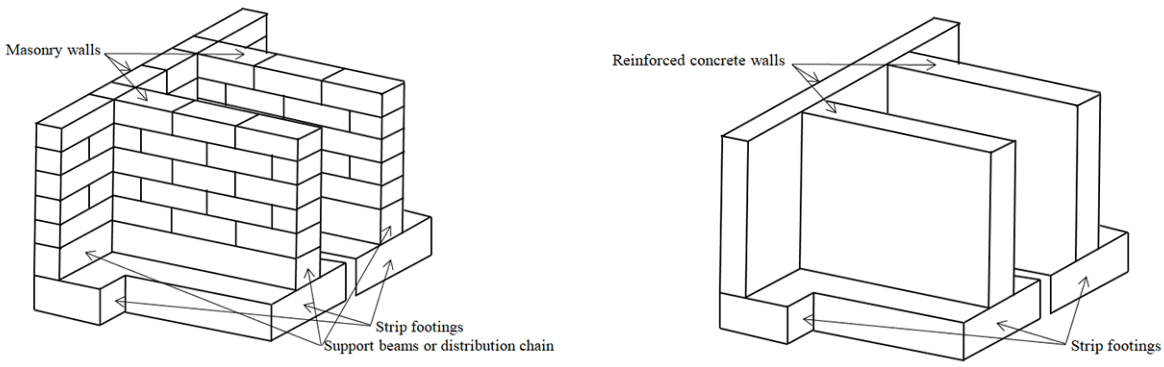

(a) Footing that supports masonry walls (b) Footing that supports concrete walls

FIGURE 2. Strip footing

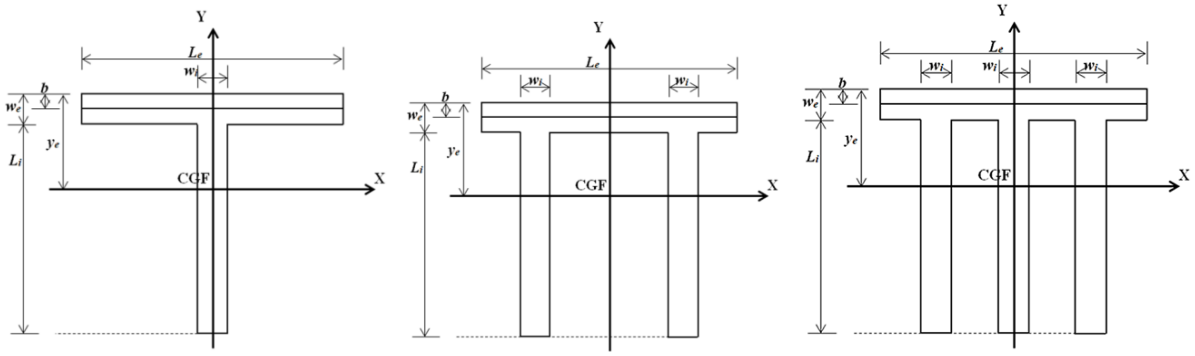

(a) One transverse footing (b) Two transverse footings (c) Three transverse footings

FIGURE 3. Border strip footing

Figure 3 indicates a border strip footing with one, two and three transverse footings.

Substituting $M_{uy} = 0$ (symmetrical walls in load and geometry with respect to the Y axis) and R_u (ultimate resultant force in kN) by P_u into Equation (1), the overall pressure is obtained:

$$p_{us} = \frac{R_u}{A} + \frac{M_{ux}y}{I_x} \tag{2}$$

where $R_u = P_{u1} + P_{u2}$, $P_{u1} = w_{u1}L_e$, $P_{u2} = nw_{u2}(L_i + w_e - b)$, w_{u1} is the ultimate load of the outer wall in kN/m, n is the number of foundations transverse to the outer foundation, and w_{u2} is the ultimate load of the inside wall in kN/m.

The ultimate moment on the X axis is [2]:

$$M_{ux} = \frac{P_{u1}(2y_e - b) + P_{u2}(L_i + w_e + b - 2y_e)}{2} \tag{3}$$

The properties of the base of a strip footing are indicated in Equations (2) to (4) of Luévanos-Soto et al. [2].

2.1. **Case I.** When the contact surface is working entirely in compression or the current model (the moment appears on the X axis and the moment does not appear on the Y axis).

Figure 4 represents the sections of case I for ultimate moments and ultimate shears acting on the footing.

2.1.1. *Ultimate moments.* The ultimate moment on the "a" axis acting on the footing is obtained:

$$M_{ua} = \frac{P_{u1}b}{2} - \int_{y_e-b}^{y_e}\int_{-\frac{L_e}{2}}^{\frac{L_e}{2}} p_{us}(y - y_e + b)dxdy \tag{4}$$

The ultimate moment on the "b" axis acting on the footing is determined:

$$M_{ub} = \frac{P_{u1}(2w_e - b)}{2} + \frac{nw_{u2}(w_e - b)^2}{2} - \int_{y_e-w_e}^{y_e}\int_{-\frac{L_e}{2}}^{\frac{L_e}{2}} p_{us}(y - y_e + w_e)dxdy \tag{5}$$

The ultimate moment on the "f" axis acting on the footing is obtained:

$$M_{uf} = \frac{P_{u1}(2L_i + 2w_e - b)}{2} + \frac{nw_{u2}(L_i + w_e - b)(3L_i + 3w_e + b - 4y_e)}{2} - \int_{y_e-w_e}^{y_e}\int_{-\frac{L_e}{2}}^{\frac{L_e}{2}} p_{us}(y - y_e + L_i + w_e)dxdy$$

$$- n \int_{y_e - L_i - w_e}^{y_e - w_e} \int_{-\frac{w_i}{2}}^{\frac{w_i}{2}} p_{us}(y - y_e + L_i + w_e) dxdy \tag{6}$$

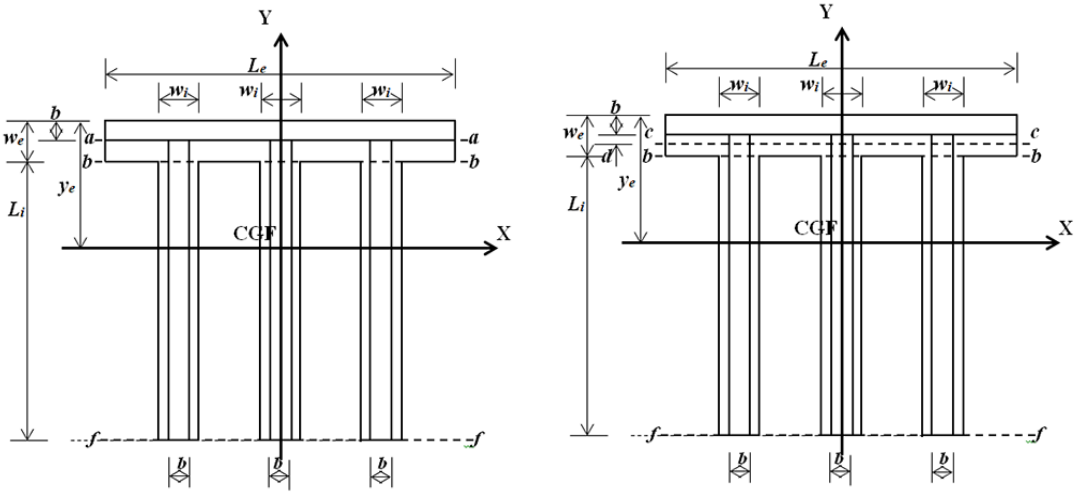

(a) Ultimate moments (b) Ultimate shears

FIGURE 4. Critical sections of case I for moments and shears

Also, it can be expressed as follows:

$$\begin{aligned} M_{uf} = & \frac{P_{u1}(2L_i + 2w_e - b)}{2} + \frac{P_{u2}(3L_i + 3w_e + b - 4y_e)}{2} \\ & - \int_{y_e - w_e}^{y_e} \int_{-\frac{L_e}{2}}^{\frac{L_e}{2}} p_{us}(y - y_e + L_i + w_e) dxdy \\ & - n \int_{y_e - L_i - w_e}^{y_e - w_e} \int_{-\frac{w_i}{2}}^{\frac{w_i}{2}} p_{us}(y - y_e + L_i + w_e) dxdy \end{aligned} \tag{7}$$

2.1.2. *Ultimate bending shears.* The ultimate bending shear on the "c" axis acting on the footing is obtained:

$$V_{uc} = P_{u1} + n w_{u2} d - \int_{y_e - b - d}^{y_e} \int_{-\frac{L_e}{2}}^{\frac{L_e}{2}} p_{us} dxdy \tag{8}$$

where d is the effective depth of the foundation.

The ultimate bending shear on the "b" axis acting on the footing is obtained:

$$V_{ub} = P_{u1} + n w_{u2}(w_e - b) - \int_{y_e - w_e}^{y_e} \int_{-\frac{L_e}{2}}^{\frac{L_e}{2}} p_{us} dxdy \tag{9}$$

The ultimate bending shear on the "f" axis acting on the footing is determined:

$$V_{uf} = P_{u1} + n w_{u2}(L_i + w_e - b) - \int_{y_e - w_e}^{y_e} \int_{-\frac{L_e}{2}}^{\frac{L_e}{2}} p_{us} dxdy - n \int_{y_e - L_i - w_e}^{y_e - w_e} \int_{-\frac{w_i}{2}}^{\frac{w_i}{2}} p_{us} dxdy \tag{10}$$

Also, it can be expressed as follows:

$$V_{uf} = P_{u1} + P_{u2} - \int_{y_e - w_e}^{y_e} \int_{-\frac{L_e}{2}}^{\frac{L_e}{2}} p_{us} dxdy - n \int_{y_e - L_i - w_e}^{y_e - w_e} \int_{-\frac{w_i}{2}}^{\frac{w_i}{2}} p_{us} dxdy \tag{11}$$

2.2. **Case II.** When the contact surface is working partially in compression, the neutral axis falls inside the flanges, i.e., $w_y \leq w_e$ (the moment appears on the X axis and the moment does not appear on the Y axis).

The ultimate pressure at any point of the footing "p_{uz}" using Equation (9) of Luévanos-Soto et al. [2] is determined:

$$p_{uz} = \frac{p_{us\max}(w_y - y_e + y)}{w_y} \tag{12}$$

where $p_{us\max}$ is the ultimate maximum pressure in kN/m^2, and y is the coordinate of the foundation on the Y axis in m.

Figure 5 represents the sections of case II for ultimate moments and ultimate shears acting on the footing.

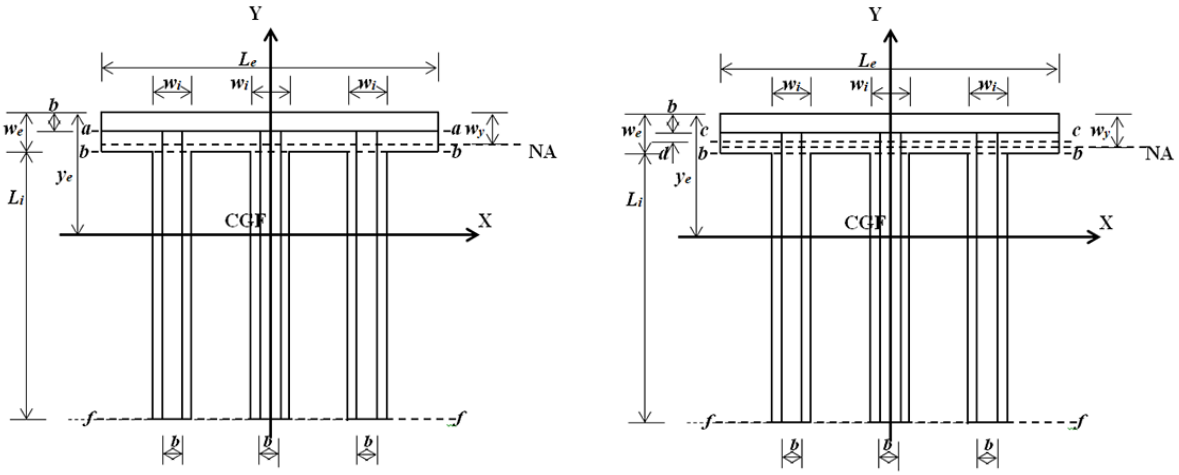

(a) Ultimate moments (b) Ultimate shears

FIGURE 5. Critical sections of case II for moments and shears

2.2.1. *Ultimate moments.* The ultimate moment on the "a" axis acting on the footing is obtained:

$$M_{ua} = \frac{P_{u1}b}{2} - \int_{y_e-b}^{y_e}\int_{-\frac{L_e}{2}}^{\frac{L_e}{2}} p_{uz}(y - y_e + b)dxdy \tag{13}$$

The ultimate moment on the "f" axis acting on the footing is obtained:

$$M_{uf} = \frac{P_{u1}(2w_y - b)}{2} + \frac{nw_{u2}(L_i + w_e - b)(2w_y - L_i - w_e + b)}{2} - \int_{y_e-w_y}^{y_e}\int_{-\frac{L_e}{2}}^{\frac{L_e}{2}} p_{uz}(y - y_e + w_y)dxdy \tag{14}$$

Also, it can be expressed as follows:

$$M_{uf} = \frac{P_{u1}(2w_y - b)}{2} + \frac{P_{u2}(2w_y - L_i - w_e + b)}{2} - \int_{y_e-w_y}^{y_e}\int_{-\frac{L_e}{2}}^{\frac{L_e}{2}} p_{uz}(y - y_e + w_y)dxdy \tag{15}$$

2.2.2. *Ultimate bending shears.* The ultimate bending shear on the "c" axis acting on the footing is obtained:

$$V_{uc} = P_{u1} + nw_{u2}d - \int_{y_e-b-d}^{y_e} \int_{-\frac{L_e}{2}}^{\frac{L_e}{2}} p_{uz} dxdy \tag{16}$$

The ultimate bending shear on the "f" axis acting on the footing is determined:

$$V_{uf} = P_{u1} + nw_{u2}(w_y - b) - \int_{y_e-w_y}^{y_e} \int_{-\frac{L_e}{2}}^{\frac{L_e}{2}} p_{uz} dxdy \tag{17}$$

Also, it can be expressed as follows:

$$V_{uf} = P_{u1} + P_{u2} - \int_{y_e-w_y}^{y_e} \int_{-\frac{L_e}{2}}^{\frac{L_e}{2}} p_{uz} dxdy \tag{18}$$

2.3. **Case III.** When the contact surface is working partially in compression, the neutral axis falls inside the web, i.e., $w_y \geq w_e$ (the moment appears on the X axis and the moment does not appear on the Y axis).

Figure 6 represents the sections of case III for ultimate moments and ultimate shears acting on the footing.

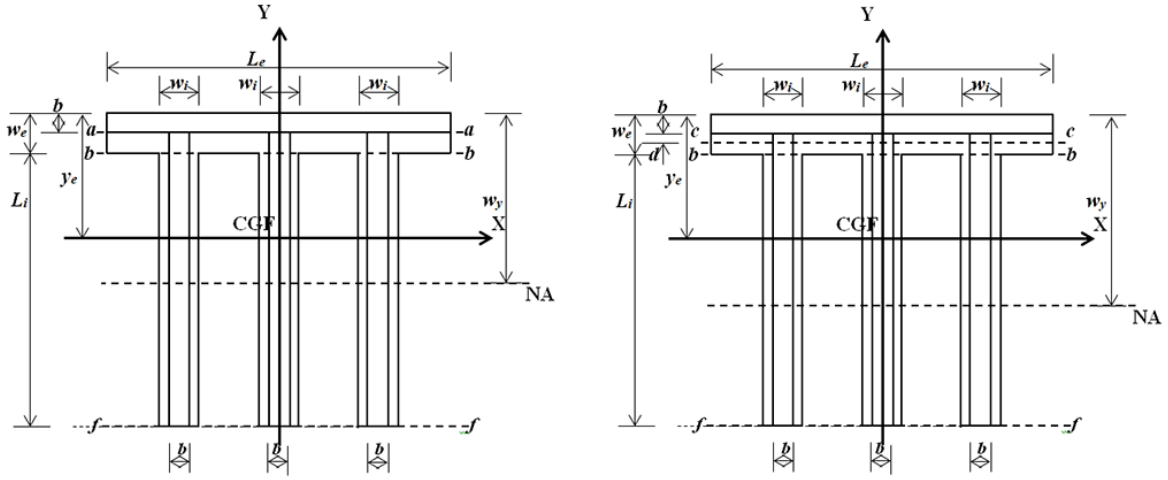

(a) Ultimate moments (b) Ultimate shears

FIGURE 6. Critical sections of case III for moments and shears

2.3.1. *Ultimate moments.* The ultimate moment on the "a" axis acting on the footing is obtained:

$$M_{ua} = \frac{P_{u1}b}{2} - \int_{y_e-b}^{y_e} \int_{-\frac{L_e}{2}}^{\frac{L_e}{2}} p_{uz}(y - y_e + b) dxdy \tag{19}$$

The ultimate moment on the "b" axis acting on the footing is determined:

$$M_{ub} = \frac{P_{u1}(2w_e - b)}{2} + \frac{nw_{u2}(w_e - b)^2}{2} - \int_{y_e-w_e}^{y_e} \int_{-\frac{L_e}{2}}^{\frac{L_e}{2}} p_{uz}(y - y_e + w_e) dxdy \tag{20}$$

The ultimate moment on the "f" axis acting on the footing is obtained:

$$M_{uf} = \frac{P_{u1}(2L_i + 2w_e - b)}{2} + \frac{nw_{u2}(L_i + w_e - b)(3L_i + 3w_e + b - 4y_e)}{2} - \int_{y_e-w_e}^{y_e} \int_{-\frac{L_e}{2}}^{\frac{L_e}{2}} p_{uz}(y - y_e + L_i + w_e) dxdy$$

$$- n \int_{y_e - w_y}^{y_e - w_e} \int_{-\frac{w_i}{2}}^{\frac{w_i}{2}} p_{uz}(y - y_e + L_i + w_e) dx dy \tag{21}$$

Also, it can be expressed as follows:

$$\begin{aligned} M_{uf} = & \frac{P_{u1}(2L_i + 2w_e - b)}{2} + \frac{P_{u2}(3L_i + 3w_e + b - 4y_e)}{2} \\ & - \int_{y_e - w_e}^{y_e} \int_{-\frac{L_e}{2}}^{\frac{L_e}{2}} p_{uz}(y - y_e + L_i + w_e) dx dy \\ & - n \int_{y_e - w_y}^{y_e - w_e} \int_{-\frac{w_i}{2}}^{\frac{w_i}{2}} p_{uz}(y - y_e + L_i + w_e) dx dy \end{aligned} \tag{22}$$

2.3.2. *Ultimate bending shears.* The ultimate bending shear on the "c" axis acting on the footing is obtained:

$$V_{uc} = P_{u1} + n w_{u2} d - \int_{y_e - b - d}^{y_e} \int_{-\frac{L_e}{2}}^{\frac{L_e}{2}} p_{uz} dx dy \tag{23}$$

The ultimate bending shear on the "b" axis acting on the footing is obtained:

$$V_{ub} = P_{u1} + n w_{u2}(w_e - b) - \int_{y_e - w_e}^{y_e} \int_{-\frac{L_e}{2}}^{\frac{L_e}{2}} p_{uz} dx dy \tag{24}$$

The ultimate bending shear on the "f" axis acting on the footing is determined:

$$V_{uf} = P_{u1} + n w_{u2}(L_i + w_e - b) - \int_{y_e - w_e}^{y_e} \int_{-\frac{L_e}{2}}^{\frac{L_e}{2}} p_{uz} dx dy - n \int_{y_e - w_y}^{y_e - w_e} \int_{-\frac{w_i}{2}}^{\frac{w_i}{2}} p_{uz} dx dy \tag{25}$$

Also, it can be expressed as follows:

$$V_{uf} = P_{u1} + P_{u2} - \int_{y_e - w_e}^{y_e} \int_{-\frac{L_e}{2}}^{\frac{L_e}{2}} p_{uz} dx dy - n \int_{y_e - w_y}^{y_e - w_e} \int_{-\frac{w_i}{2}}^{\frac{w_i}{2}} p_{uz} dx dy \tag{26}$$

2.4. **Optimal cost design for a strip footing.**

2.4.1. *Objective.* The equation to obtain the optimal cost "C_{op}" for the three cases is

$$C_{op} = V_c C_c + V_s \gamma_s C_s \tag{27}$$

where V_c is the volume of concrete in m^3, C_s is the cost of steel in USD/kN, V_s is the volume of steel in m^3, and γ_s is the density of steel = 78 $\mathrm{kN/m}^3$.

The reinforcing steel of a strip footing is constructed in one Y direction "A_{sy}" and in the other X direction "A_{sx}".

The volume of reinforcing steel is

$$V_s = w_e A_{sya} + n L_i A_{syb} + L_e A_{sx1} + n w_i A_{sx2} \tag{28}$$

where A_{sya} is the steel area in Y direction on "a" axis, A_{syb} is the steel area in Y direction on "b" axis, A_{sx1} is the steel area by temperature in X direction with a width "w_e", and A_{sx2} is the steel area by temperature in X direction with a width "L_i".

The volume of concrete is

$$V_c = (w_e L_e + n w_i L_i)(d + r) - [w_e A_{sya} + n L_i A_{syb} + L_e A_{sx1} + n w_i A_{sx2}] \tag{29}$$

where r is the concrete cover.

Substituting V_s, V_c and γ_s into Equation (27) gives

$$C_{op} = \{(w_e L_e + n w_i L_i)(d + r) - [w_e A_{sya} + n L_i A_{syb} + L_e A_{sx1} + n w_i A_{sx2}]\} C_c$$

$$+ [w_e A_{sya} + nL_i A_{syb} + L_e A_{sx1} + nw_i A_{sx2}]\gamma_s C_s \tag{30}$$

Now, substituting $\beta = \gamma_s C_s / C_c \rightarrow \gamma_s C_s = \beta C_c$ into Equation (30) gives

$$C_{op} = (w_e L_e + nw_i L_i)(d + r)C_c - [w_e A_{sya} + nL_i A_{syb} + L_e A_{sx1} + nw_i A_{sx2}](1 - \beta)C_c \tag{31}$$

2.4.2. *Constraints.* Simplified equations for foundations design according to the American Concrete Institute standard code are shown below [60].

For moments:

$$|M_{ua}| \leq \emptyset_f f_y d A_{sya} \left(1 - \frac{A_{sya} f_y}{1.7 L_e d f'_c}\right) \tag{32}$$

$$\left|\frac{M_{ub}}{n}\right| \leq \emptyset_f f_y d A_{syb} \left(1 - \frac{A_{syb} f_y}{1.7 w_i d f'_c}\right) \tag{33}$$

where f_y is the specified yield strength of steel in MPa, f'_c is the specified compressive strength of the concrete at 28 days in MPa, and $\emptyset_f$ is the bending strength reduction factor = 0.90.

For bending shears:

$$|V_{uc}| \leq 0.17 \emptyset_v \sqrt{f'_c} L_e d \tag{34}$$

$$\left|\frac{V_{ue}}{n}\right| \leq 0.17 \emptyset_v \sqrt{f'_c} w_i d \tag{35}$$

where $\emptyset_v$ is the shear strength reduction factor = 0.85.

For steel percentages:

$$\frac{\dfrac{0.25\sqrt{f'_c}}{f_y}}{\dfrac{1.4}{f_y}} \leq \rho_a, \rho_b \leq 0.75 \left[\frac{0.85\beta_1 f'_c}{f_y}\left(\frac{600}{600 + f_y}\right)\right] \tag{36}$$

$$0.65 \leq \beta_1 = \left(1.05 - \frac{f'_c}{140}\right) \leq 0.85 \tag{37}$$

where ρ_a is the percentage of steel in "a" section with a width "L_e", and ρ_b is the percentage of steel in "b" section with a width "w_i".

For steel areas:

$$A_{sya} = \rho_a L_e d \tag{38}$$

$$A_{syb} = \rho_a w_i d \tag{39}$$

$$A_{sx1} = 0.0018 w_e d \tag{40}$$

$$A_{sx2} = 0.0018 L_i d \tag{41}$$

Note: Equations (40) and (41) are given by temperature because no bending occurs in these sections according to the ACI code [60].

Figure 7 shows the flowchart for determining the minimum cost of a strip footing for the three cases using Maple software (Nonlinear optimization).

The general procedure to obtain the minimum cost is used as follows.

The first stage is to obtain the minimum area using the procedure proposed by Luévanos-Soto et al. [2].

The second stage is to use the procedure described in this paper to obtain the minimum cost using the Maple software shown in Figure 7.

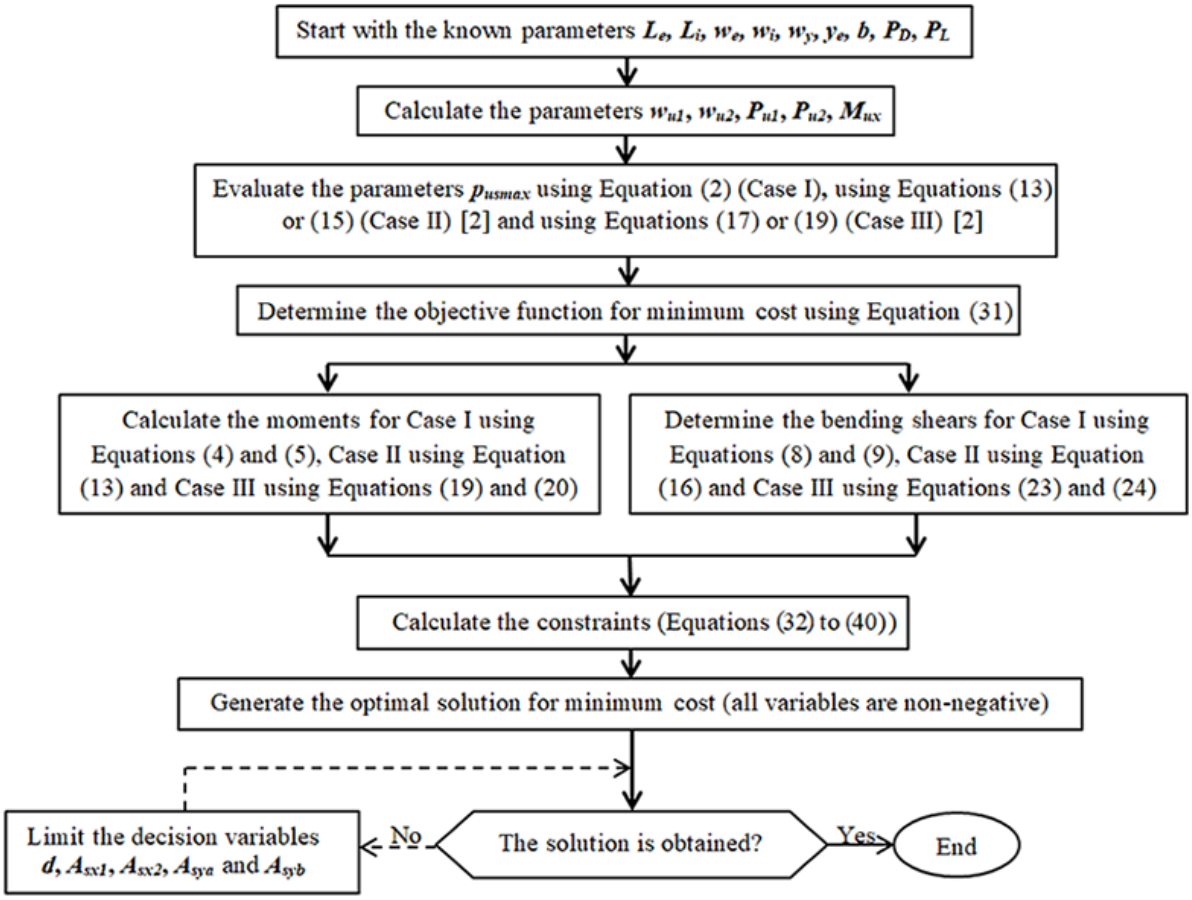

FIGURE 7. Flowchart for minimum cost of a strip footing

3. **Numerical Problems.** Four numerical studies are shown to determine the thickness, the steel area "A_{sya}", "A_{syb}", A_{sx1}" and "A_{sx2}" of a strip footing. The general data for all studies are $p_{\max} = 200$ kN/m^2; $n = 1, 2$ and 3; $L_e = 10.00$ m; $b = 0.30$ m; $r = 0.08$ m, $f'_c = 21$ MPa, $f_y = 420$ MPa and $\beta = 90$. Study 1 ($w_e \neq w_i$) and Study 2 ($w_e = w_i$) are developed for $w_1 = w_2 = 120$ kN/m ($w_{D1} = w_{D2} = 50$ kN/m and $w_{L1} = w_{L2} = 70$ kN/m). Study 3 ($w_e \neq w_i$) and Study 4 ($w_e = w_i$) are developed for $w_1 = w_2 = 40$ kN/m ($w_{D1} = w_{D2} = 15$ kN/m and $w_{L1} = w_{L2} = 25$ kN/m). These studies are based on examples 1 to 4 of the data presented in the article proposed by Luévanos-Soto et al. [2].

The uniformly distributed ultimate load is $w_{u1} = w_{u2} = 1.2(50) + 1.6(70) = 172$ kN/m (Studies 1 and 2) and $w_{u1} = w_{u2} = 1.2(15) + 1.6(25) = 58$ kN/m (Studies 3 and 4).

Tables 1 to 4 represent the P_{u1} (ultimate load due to the outer wall), P_{u2} (ultimate load due to the inside wall), M_{ux} (ultimate moment on the X axis), $p_{us\max}$ (ultimate maximum pressure), y_e (distance from center of footing to outer edge), d (effective depth of the footing), A_{sx1} (steel area by temperature in X direction with a width "w_e"), A_{sx2} (steel area by temperature in X direction with a width "L_i"), A_{sya} (steel area in Y direction on "a" axis with a width "L_e"), A_{syb} (steel area in Y direction on "b" axis with a width "w_i"), ρ_a (percentage of steel in "a" section with a width "L_e"), ρ_b (percentage of steel in "b" section with a width "w_i"), C_{op} (optimal or minimum cost based on the cost of concrete).

Table 1 indicates the final design of Study 1 based on Table 2 of Luévanos-Soto et al. [2].

TABLE 1. Final design for $w_e \neq w_i$, $w_{D1} = w_{D2} = 50$ kN/m and $w_{L1} = w_{L2} = 70$ kN/m

Case	n	P_{u1} (kN)	P_{u2} (kN)	M_{ux} (kN-m)	$p_{us\max}$ (kN/m^2)	y_e (cm)	d (cm)	A_{sx1} (cm^2)	A_{sx2} (cm^2)	A_{sya} (cm^2)	A_{syb} (cm^2)	ρ_a	ρ_b	C_{op} (USD)
I	1	1720	3703.16	20727.30	286.68	10.08	82.46	4.76	319.23	274.59	40.77	0.00333	0.00333	$45.02C_c$
II		1720	577.53	2974.27	286.67	1.83	15.00	9.88	0	49.95	0	0.00333	$*$	$10.92C_c$
III		1720	870.07	4083.57	286.67	2.21	15.00	2.14	12.33	49.95	61.61	0.00333	0.01126	$9.10C_c$
I	2	1720	3597.05	9532.19	98.86	5.38	19.75	38.01	0.22	65.75	79.87	0.00333	0.00809	$39.59C_c$
II		1720	1005.50	2974.27	286.67	1.61	15.00	8.70	0	49.95	0	0.00333	$*$	$9.62C_c$
III		1720	1636.25	4305.55	286.67	2.16	15.00	2.28	11.37	49.95	26.67	0.00333	0.00801	$9.27C_c$
I	3	1720	3677.19	6680.23	145.35	3.71	50.06	66.91	0	166.69	0	0.00333	$*$	$60.09C_c$
II		1720	1480.66	2689.87	286.67	1.58	15.00	6.03	2.53	49.95	58.44	0.00333	0.01169	$10.51C_c$
III		1720	1960.30	3598.68	286.67	1.89	15.00	2.33	8.74	49.95	17.90	0.00333	0.00539	$9.58C_c$

where $*$ indicates that there is no ρ_b, because there is no reinforcing steel, since the footing is rectangular.

Table 2 indicates the final design of Study 2 based on Table 3 of Luévanos-Soto et al. [2].

TABLE 2. Final design for $w_e = w_i$, $w_{D1} = w_{D2} = 50$ kN/m and $w_{L1} = w_{L2} = 70$ kN/m

Case	n	P_{u1} (kN)	P_{u2} (kN)	M_{ux} (kN-m)	$p_{us\max}$ (kN/m^2)	y_e (cm)	d (cm)	A_{sx1} (cm^2)	A_{sx2} (cm^2)	A_{sya} (cm^2)	A_{syb} (cm^2)	ρ_a	ρ_b	C_{op} (USD)
I	1	1720	3517.97	18117.56	50.48	10.38	28.05	50.49	54.29	93.40	447.08	0.00333	0.00333	$135.24C_c$
II		1720	577.53	2974.27	286.67	1.83	15.00	9.88	0	49.95	0	0.00333	$*$	$10.92C_c$
III		1720	1885.23	10049.82	286.67	3.57	150.55	43.39	261.32	501.34	80.28	0.00333	0.00333	$71.55C_c$
I	2	1720	3597.05	9532.19	98.86	5.38	19.75	17.78	20.46	65.75	135.84	0.00333	0.01376	$50.09C_c$
II		1720	1005.50	2664.58	286.67	1.61	15.00	8.70	0	49.95	0	0.00333	$*$	$9.62C_c$
III		1720	2510.95	7453.01	286.67	2.79	79.12	19.37	8.88	263.46	35.84	0.00333	0.00333	$37.69C_c$
I	3	1720	3677.19	6680.23	145.35	3.71	17.27	10.36	12.73	57.52	56.74	0.00333	0.00985	$28.73C_c$
II		1720	1480.66	2689.87	286.67	1.58	15.00	8.56	0	49.95	0	0.00333	$*$	$9.46C_c$
III		1720	1759.81	3201.99	286.67	1.73	25.11	10.97	5.80	83.60	20.30	0.00333	0.00333	$14.98C_c$

Table 3 indicates the final design of Study 3 based on Table 4 of Luévanos-Soto et al. [2].

TABLE 3. Final design for $w_e \neq w_i$, $w_{D1} = w_{D2} = 15$ kN/m and $w_{L1} = w_{L2} = 25$ kN/m

Case	n	P_{u1} (kN)	P_{u2} (kN)	M_{ux} (kN-m)	$p_{us\max}$ (kN/m^2)	y_e (cm)	d (cm)	A_{sx1} (cm^2)	A_{sx2} (cm^2)	A_{sya} (cm^2)	A_{syb} (cm^2)	ρ_a	ρ_b	C_{op} (USD)
I	1	580	0	0	193.33	0.15	15.00	0.81	0	49.95	0	0.00333	$*$	$0.90C_c$
II		580	25.69	42.17	290.00	0.21	15.00	1.13	0	49.95	0	0.00333	$*$	$1.25C_c$
III		580	32.19	26.07	290.00	0.17	15.00	0.81	1.50	49.95	3.36	0.00333	0.00747	$0.95C_c$
I	2	580	0	0	193.33	0.15	15.00	0.81	0	49.95	0	0.00333	$*$	$0.90C_c$
II		580	34.06	47.63	290.00	0.22	15.00	1.14	0.46	49.95	1.50	0.00333	0.00333	$1.29C_c$
III		580	40.05	24.17	290.00	0.17	15.00	0.81	0.93	49.95	1.64	0.00333	0.00364	$0.96C_c$
I	3	580	0	0	193.33	0.15	15.00	0.81	0	49.95	0	0.00333	$*$	$0.90C_c$
II		580	38.71	47.20	290.00	0.22	15.00	1.15	0.26	49.95	1.50	0.00333	0.00333	$1.30C_c$
III		580	43.94	22.57	290.00	0.17	15.00	0.81	0.68	49.95	1.50	0.00333	0.00333	$0.96C_c$

Table 4 indicates the final design of Study 4 based on Table 5 of Luévanos-Soto et al. [2].

TABLE 4. Final design for $w_e = w_i$, $w_{D1} = w_{D2} = 15$ kN/m and $w_{L1} = w_{L2} = 25$ kN/m

Case	n	P_{u1} (kN)	P_{u2} (kN)	M_{ux} (kN-m)	$p_{us\max}$ (kN/m^2)	y_e (cm)	d (cm)	A_{sx1} (cm^2)	A_{sx2} (cm^2)	A_{sya} (cm^2)	A_{syb} (cm^2)	ρ_a	ρ_b	C_{op} (USD)
I	1	580	1186.29	6109.41	17.02	10.38	16.29	29.32	31.53	54.24	259.62	0.00333	0.01594	$85.49C_c$
II		580	26.83	50.02	290.00	0.22	15.00	1.13	0.93	49.95	2.21	0.00333	0.00351	$1.29C_c$
III		580	32.19	26.07	290.00	0.17	15.00	0.81	1.50	49.95	3.36	0.00333	0.00747	$0.95C_c$
I	2	580	1212.96	3214.34	33.34	5.38	15.00	13.50	15.54	49.95	55.32	0.00333	0.00738	$35.22C_c$
II		580	34.57	49.60	290.00	0.22	15.00	1.14	0.47	49.95	2.12	0.00333	0.00333	$1.31C_c$
III		580	40.05	24.17	290.00	0.17	15.00	0.81	0.93	49.95	1.64	0.00333	0.00364	$0.96C_c$
I	3	580	1239.98	2252.64	49.01	3.71	15.00	9.00	11.05	49.95	20.46	0.00333	0.00409	$22.58C_c$
II		580	39.25	48.75	290.00	0.22	15.00	1.15	0.27	49.95	2.13	0.00333	0.00333	$1.31C_c$
III		580	43.94	22.57	290.00	0.17	15.00	0.81	0.68	49.95	1.50	0.00333	0.00333	$0.96C_c$

4. **Results.** Tables 1 to 4 are the data based on Tables 2 to 5 of Luévanos-Soto et al. [2].

Table 1 shows the following: For $n = 1$ when cases increase, P_{u2}, M_{ux}, y_e, A_{sx2}, A_{syb} and ρ_b (case II does not show ρ_b) tend to decrease and then increase, $p_{us\max}$, d and A_{sya} in cases II and III are equal, A_{sx1} tends to increase and then decrease, P_{u1} and ρ_a are equal, while C_{op} decreases. For $n = 2$ when cases increase, P_{u2}, M_{ux}, y_e, A_{sx2}, A_{syb} and ρ_b (case II does not show ρ_b) tend to decrease and then increase, $p_{us\max}$, d and A_{sya} in cases II and III are equal, P_{u1} and ρ_a are equal, while A_{sx1} and C_{op} decrease. For $n = 3$ when cases increase, P_{u2}, M_{ux} and y_e tend to decrease and then increase, A_{sx2} increases, A_{syb} and ρ_b (case I does not show ρ_b) tend to increase and then decrease, $p_{us\max}$, d and A_{sya} in cases II and III are equal, P_{u1} and ρ_a are equal, while A_{sx1} and C_{op} decrease. For all values of n, the lowest cost appears in case III.

Table 2 presents the following: For $n = 1$ when cases increase, P_{u2}, M_{ux}, y_e, A_{sx1}, A_{sx2}, A_{sya}, A_{syb}, d and ρ_b (Cases I and III are the same, and Case II is not shown ρ_b) tend to decrease and then increase, $p_{us\max}$ in cases II and III are equal, P_{u1} and ρ_a are equal, while C_{op} decreases and then increases. For $n = 2$ the same trends appear as for $n = 1$. For $n = 3$, the same trends appear as for $n = 1$. For all values of n, the lowest cost appears in case II.

Table 3 shows the following: For $n = 1$ when cases increase, M_{ux}, y_e and A_{sx1} tend to increase and then decrease, A_{sx2} and A_{syb} are equal to zero (Cases I and II), ρ_b (Cases I and II no show value), P_{u2} increases, $p_{us\max}$ in cases II and III is equal, P_{u1}, d, A_{sya} and ρ_a are equal, while C_{op} increases and then decreases. For $n = 2$ when cases increase, M_{ux}, y_e and A_{sx1} tend to increase and then decrease, P_{u2}, A_{sx2}, A_{syb} and ρ_b (case I does not show ρ_b) tend to increase, $p_{us\max}$ in cases II and III is equal, P_{u1}, d, A_{sya} and ρ_a are equal, while C_{op} increases and then decreases. For $n = 3$ when cases increase, M_{ux}, y_e and A_{sx1} tend to increase and then decrease, P_{u2} and A_{sx2} tend to increase, $p_{us\max}$, A_{syb} and ρ_b (case I does not show ρ_b) in cases II and III are equal, P_{u1}, d, A_{sya} and ρ_a are equal, while C_{op} increases and then decreases. For all values of n, the lowest cost appears in case I.

Table 4 presents the following: For $n = 1$ when cases increase, M_{ux}, y_e and A_{sx1} tend to decrease, P_{u2}, A_{sx2}, A_{syb} and ρ_b tend to decrease and then increase, $p_{us\max}$, A_{sya} and d in cases II and III are equal, P_{u1} and ρ_a are equal, while C_{op} decreases. For $n = 2$ when cases increase, M_{ux}, y_e, A_{sx1} and A_{syb} tend to decrease, P_{u2}, A_{sx2} and ρ_b tend to decrease and then increase, $p_{us\max}$ in cases II and III is equal, P_{u1}, d, A_{sya} and ρ_a are equal, while C_{op} decreases. For $n = 3$ when cases increase, M_{ux}, y_e, A_{sx1} and A_{syb} tend to decrease, P_{u2} and A_{sx2} tend to decrease and then increase, $p_{us\max}$ and ρ_b in cases II and III are

equal, P_{u1}, d, A_{sya} and ρ_a are equal, while C_{op} decreases. For all values of n, the lowest cost appears in case III.

Important note: The moments "M_{uf}" and the bending shears "V_{uf}" in section f are shown to verify the continuity of all the equations because in this section they must be zero.

Figure 8 shows in detail the dimensions and the steel of a general shape for a strip foundation.

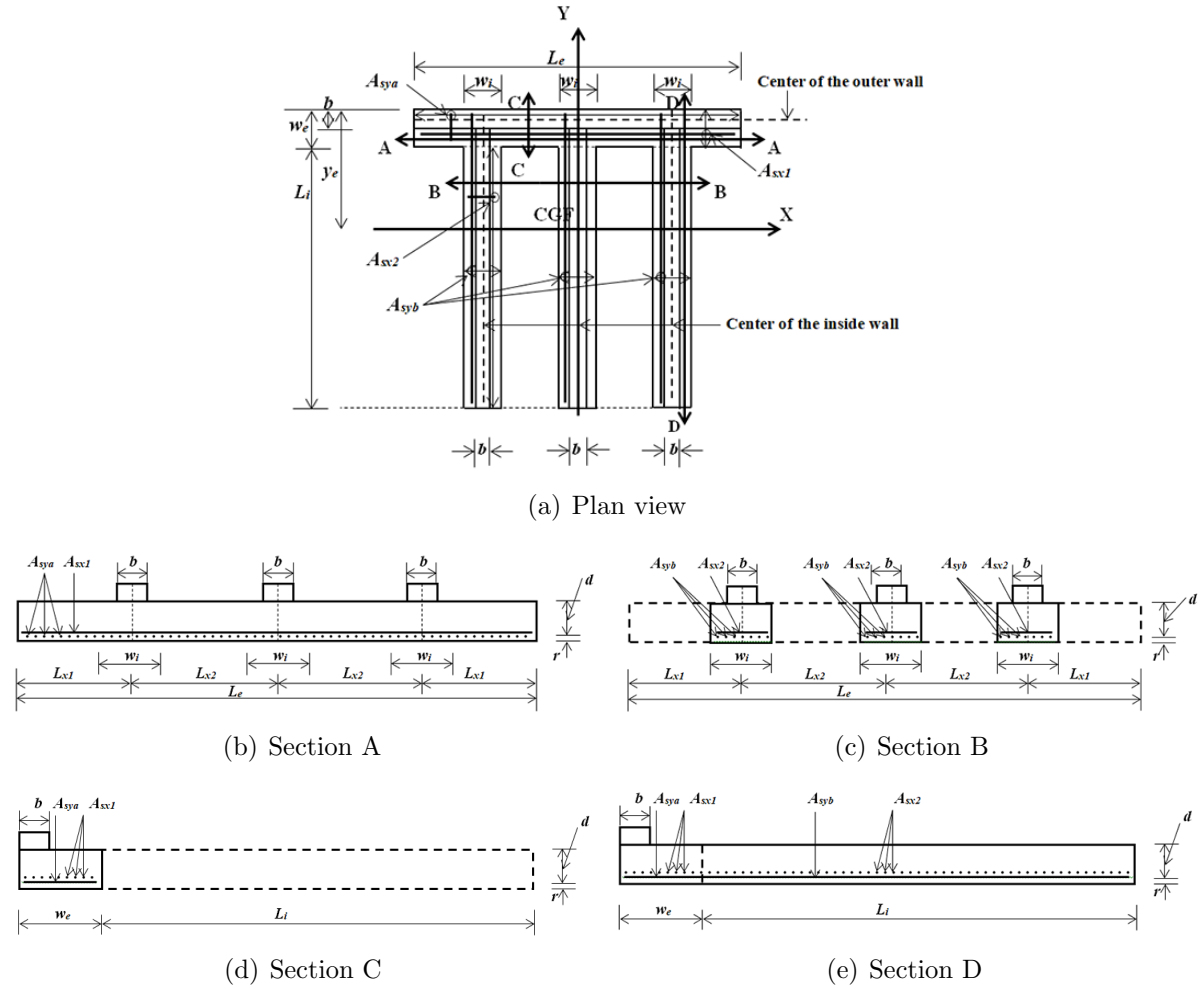

(a) Plan view

(b) Section A

(c) Section B

(d) Section C

(e) Section D

FIGURE 8. Diagram of a strip foundation

Figure 9 presents the minimum or optimal cost for a strip foundation of the four studies for the three cases. Case I is the current model, and Cases II and III are the models presented in this work.

Figure 9(a) shows a saving of 75.74% in Case II and 79.79% in Case III for $n = 1$, for $n = 2$ they present a saving of 75.70% in Case II and 76.58% in Case III, and for $n = 3$ they show a saving of 82.51% in Case II and 84.06% in Case III with respect to Case I. Therefore, the greatest savings occur in case III for $n = 3$.

Figure 9(b) presents a saving of 91.93% in Case II and 47.09% in Case III for $n = 1$, for $n = 2$ they present a saving of 80.79% in Case II and 24.76% in Case III, and for $n = 3$ they show a saving of 67.07% in Case II and 47.86% in Case III with respect to Case I. Therefore, the greatest savings occur in case II for $n = 1$.

Figure 9(c) shows increases of 1.39 times in Case II and 1.06 times in Case III for $n = 1$, for $n = 2$ they present a saving of 1.43 times in Case II and 1.07 times in Case III, and

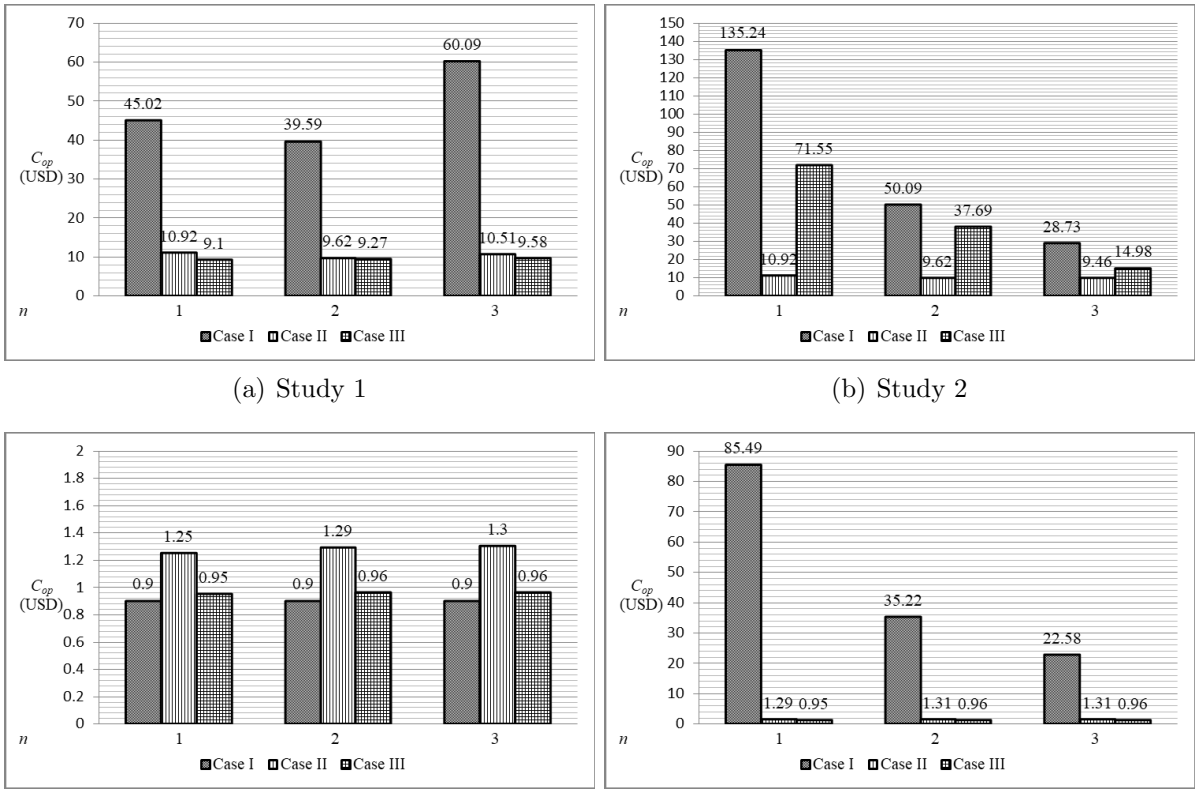

(a) Study 1 (b) Study 2

(c) Study 3 (d) Study 4

FIGURE 9. Minimum or optimal cost for a strip foundation

for $n = 3$ they show a saving of 1.44 times in Case II and 1.07 in Case III with respect to Case I. Therefore, the greatest savings occur in case I for $n = 3$.

Figure 9(d) presents a saving of 98.49% in Case II and 98.89% in Case III for $n = 1$, for $n = 2$ they present a saving of 96.28% in Case II and 97.27% in Case III, and for $n = 3$ they show a saving of 94.20% in Case II and 95.75% in Case III with respect to Case I. Therefore, the greatest savings occur in case III for $n = 1$.

5. **Conclusions.** This paper shows a model to determine the minimum or optimal design cost for a strip footing to obtain the longitudinal and transverse steel area, the thickness, assuming that the soil is elastic, the distribution of soil pressures is linear and the surface in contact with the soil is partially compressed.

This model is based on parameters known as $A_{\min}$, L_e, L_i, P_D, P_L, w_e, w_i, w_y and y_e proposed by Luévanos-Soto et al. [2].

The contributions of this work are as follows.

1) Some studies assume a constant soil pressure beneath the foundation because the wall is located at the center of the base, but they do not take account of the property lines that may appear in many cases (Area works entirely under compression).

2) The new model shows a great saving in case III for $n = 3$ of 84.06% compared to the current model for different foundation widths "$w_e \neq w_i$".

3) The new model presents a great saving in case III for $n = 3$ of 98.89% compared to the current model for equal foundation widths "$w_e = w_i$".

4) When the pressure generated by the soil on the contact surface of foundation is uniform or constant, case I presents the greatest savings as shown in Table 3 and Figure 9(c).

5) The imposed parameters, such as the resistance of the materials f'_c and f_y, influence as follows: for f'_c, the greater the resistance, the less the thickness; for f_y, the greater the steel resistance, the smaller the steel areas.

The suggestions for the next research:

1) Design aids for the three models presented in this article so they can be applied without the aid of software.

2) Minimum or optimal area and minimum or optimal design cost for strip footings resting on sandy or clay soils for greater accuracy, since the pressure is not linear as shown in Figure 1(a) and Figure 1(b).

REFERENCES

[1] J. E. Bowles, *Foundation Analysis and Design*, McGraw-Hill, New York, U.S.A., 2001.

[2] I. Luévanos-Soto, A. Luévanos-Rojas and R. M. Luévanos-Soto, Optimal surface in plan for strip footings assuming that the contact surface with soil works partially under compression, *International Journal of Innovative Computing, Information and Control*, vol.21, no.4, pp.937-953, 2025.

[3] J. Khazaie and S. A. Amirshahkarami, Numerical analysis of interaction between earth and large foundations regarding size effect, *Journal of Applied Sciences*, vol.9, no.6, pp.1036-1045, 2009.

[4] M. Jahanandish, M. Veiskarami and A. Ghahramani, Effect of foundation size and roughness on the bearing capacity factor, $N\gamma$, by stress level-based ZEL method, *Arabian Journal for Science and Engineering*, vol.37, no.7, pp.1817-1831, 2012.

[5] G. A. Vyacheslavovich and B. L. Adolfovich, Influence of the form and size of the isolated foundations on the stress-strain state of the soil base, *Journal of Applied Engineering Science*, vol.14, no.1, pp.28-35, 2016.

[6] S. López-Chavarría, A. Luévanos-Rojas and M. Medina-Elizondo, A mathematical model for dimensioning of square isolated footings using optimization techniques: General case, *International Journal of Innovative Computing, Information and Control*, vol.13, no.1, pp.67-74, 2017.

[7] S. López-Chavarría, A. Luévanos-Rojas and M. Medina-Elizondo, Optimal dimensioning for the corner combined footings, *Advances in Computational Design*, vol.2, no.2, pp.169-183, 2017.

[8] A. Luévanos-Rojas, A mathematical model for dimensioning of footings square, *International Review of Civil Engineering*, vol.3, no.4, pp.346-350, 2012.

[9] A. Luévanos-Rojas, A mathematical model for the dimensioning of circular footings, *Far East Journal of Mathematical Sciences*, vol.71, no.2, pp.357-367, 2012.

[10] A. Luévanos-Rojas, A mathematical model for dimensioning of footings rectangular, *ICIC Express Letters, Part B: Applications*, vol.4, no.2, pp.269-274, 2013.

[11] W. L. Filho, R. C. Carvalho, A. L. Christoforo and F. A. R. Lahr, Dimensioning of isolated footing submitted to the under biaxial bending considering the low concrete consumption, *International Journal of Materials Engineering*, vol.7, no.1, pp.1-11, 2017.

[12] A. Luévanos-Rojas, A comparative study for dimensioning of footings with respect to the contact surface on soil, *International Journal of Innovative Computing, Information and Control*, vol.10, no.4, pp.1313-1326, 2014.

[13] A. Luévanos-Rojas, A new mathematical model for dimensioning of the boundary trapezoidal combined footings, *International Journal of Innovative Computing, Information and Control*, vol.11, no.4, pp.1269-1279, 2015.

[14] A. Luévanos-Rojas, A mathematical model for the dimensioning of combined footings of rectangular shape, *Revista Técnica de la Facultad de Ingeniería Universidad del Zulia*, vol.39, no.1, pp.3-9, 2016.

[15] A. Luévanos-Rojas, S. López-Chavarría and M. Medina-Elizondo, A new model for T-shaped combined footings Part I: Optimal dimensioning, *Geomechanics and Engineering*, vol.14, no.1, pp.51-60, 2018.

[16] G. Aguilera-Mancilla, A. Luévanos-Rojas, S. López-Chavarría and M. Medina-Elizondo, Modeling for the strap combined footings Part I: Optimal dimensioning, *Steel and Composite Structures*, vol.30, no.2, pp.97-108, 2019.

[17] M. A. Moreno-Hernandez, A. Luévanos-Rojas, S. López-Chavarría and M. Medina-Elizondo, Mathematical modeling for corner strap combined footings resting on the ground: Part 1, *Computación y Sistemas*, vol.26, no.3, pp.1259-1272, 2022.

[18] M. I. L. Ávila-García, A. Luévanos-Rojas, C. Martinez-Aguilar and L. L. Gaona-Tamez, Optimal area for rectangular foundation slabs in plan supported on soil, *International Journal of Innovative Computing, Information and Control*, vol.20, no.5, pp.1399-1413, 2024.

[19] A. Luévanos-Rojas, J. G. Faudoa-Herrera, R. A. Andrade-Vallejo and M. A. Cano-Alvarez, Design of isolated footings of rectangular form using a new model, *International Journal of Innovative Computing, Information and Control*, vol.9, no.10, pp.4001-4021, 2013.

[20] S. López-Chavarría, A. Luévanos-Rojas and M. Medina-Elizondo, A new mathematical model for design of square isolated footings for general case, *International Journal of Innovative Computing, Information and Control*, vol.13, no.4, pp.1149-1168, 2017.

[21] A. Luévanos-Rojas, Design of isolated footings of circular form using a new model, *Structural Engineering and Mechanics*, vol.52, no.4, pp.767-786, 2014.

[22] A. Luévanos-Rojas, Minimum cost design for rectangular isolated footings taking into account that the column is located in any part of the footing, *Buildings*, vol.13, no.9, pp.1-16, 2023.

[23] A. Luévanos-Rojas, V. M. Moreno-Landeros, G. Santiago-Hurtado, F. J. Olguin-Coca, L. D. López-León and E. R. Diaz-Gurrola, Mathematical modeling for the optimal cost design of circular isolated footings with eccentric column, *Mathematics*, vol.12, no.5, pp.1-19, 2024.

[24] A. Luévanos-Rojas, Design of boundary combined footings of rectangular shape using a new model, *DYNA Colombia*, vol.81, no.188, pp.199-208, 2014.

[25] A. Luévanos-Rojas, A new model for the design of rectangular combined boundary footings with two restricted opposite sides, *Revista ALCONPAT*, vol.6, no.2, pp.172-187, 2016.

[26] A. Luévanos-Rojas, S. López-Chavarría and M. Medina-Elizondo, A new model for T-shaped combined footings Part II: Mathematical model for design, *Geomechanics and Engineering*, vol.14, no.1, pp.61-69, 2018.

[27] J. A. Yáñez-Palafox, A. Luévanos-Rojas, S. López-Chavarría and M. Medina-Elizondo, Modeling for the strap combined footings Part II: Mathematical model for design, *Steel and Composite Structures*, vol.30, no.2, pp.109-217, 2019.

[28] A. Luévanos-Rojas, S. López-Chavarría, M. Medina-Elizondo, R. Sandoval-Rivas and O. M. Farías-Montemayor, An analytical model for the design of corner combined footings, *Revista ALCONPAT*, vol.10, no.3, pp.317-335, 2020.

[29] M. L. Garcia-Graciano, A. Luévanos-Rojas, S. López-Chavarría and M. Medina-Elizondo, Mathematical modeling for corner strap combined footings resting on the ground: Part 2, *Computación y Sistemas*, vol.26, no.4, pp.1429-1443, 2022.

[30] A. Luévanos-Rojas, Optimization for trapezoidal combined footings: Optimal design, *Advances in Concrete Construction*, vol.16, no.1, pp.21-34, 2023.

[31] A. Luévanos-Rojas, G. Santiago-Hurtado, V. M. Moreno-Landeros, F. J. Olguin-Coca, L. D. López-León and E. R. Diaz-Gurrola, Mathematical modeling of the optimal cost for the design of strap combined footings, *Mathematics*, vol.12, no.2, pp.1-20, 2024.

[32] R. Irles-Más and F. Irles-Más, Alternativa analítica a la determinación de tensiones bajo zapatas rectangulares con flexión biaxial y despegue parcial (Explicit stresses under rectangular detached footings with biaxial bending), *Informes de la Construcción*, vol.44, no.419, pp.77-90, 1992.

[33] H. M. Algin, Stresses from linearly distributed pressures over rectangular areas, *International Journal Numerical Analytical Methods in Geomechanics*, vol.24, no.8, pp.681-692, 2000.

[34] H. M. Algin, Practical formula for dimensioning a rectangular footing, *Engineering Structures*, vol.29, no.6, pp.1128-1134, 2007.

[35] G. Özmen, Determination of base stresses in rectangular footings under biaxial bending, *Teknik Dergi Digest*, vol.22, no.4, pp.1519-1535, 2011.

[36] J. Bellos and N. P. Bakas, High computational efficiency through generic analytical formulation for linear soil pressure distribution of rigid spread rectangular footings, *Proc. of the VII European Congress on Computational Methods in Applied Sciences and Engineering*, Crete Island, Greece, 2016.

[37] J. Bellos and N. P. Bakas, Complete analytical solution for linear soil pressure distribution under rigid rectangular spread footings, *International Journal of Geomechanics*, vol.17, no.7, https://doi.org/10.1061/(ASCE)GM.1943-5622.0000874, 2017.

[38] I. Aydogdu, New iterative method to calculate base stress of footings under biaxial bending, *International Journal of Engineering & Applied Sciences (IJEAS)*, vol.8, no.4, pp.40-48, 2016.

[39] K. Girgin, Simplified formulations for the determination of rotational spring constants in rigid spread footings resting on tensionless soil, *Journal of Civil Engineering and Management*, vol.23, no.4, pp.464-474, 2017.

[40] V. B. Vela-Moreno, A. Luévanos-Rojas, S. López-Chavarría, M. Medina-Elizondo, R. Sandoval-Rivas and C. Martínez-Aguilar, Optimal area for rectangular isolated footings considering that contact surface works partially to compression, *Structural Engineering and Mechanics*, vol.84, no.4, pp.561-573, 2022.

[41] V. M. Moreno-Landeros, A. Luévanos-Rojas, G. Santiago-Hurtado, L. D. López-León and E. R. Diaz-Gurrola, Optimal area for a rectangular isolated footing with an eccentric column and partial ground compression, *Applied Sciences*, vol.14, no.15, pp.1-16, 2024.

[42] S. Soto-Garcia, A. Luévanos-Rojas, J. D. Barquero-Cabrero, S. López-Chavarría, M. Medina-Elizondo, O. M. Farias-Montemayor and C. Martínez-Aguilar, A new model for the contact surface with soil of circular isolated footings considering that the contact surface works partially under compression, *International Journal of Innovative Computing, Information and Control*, vol.18, no.4, pp.1103-1116, 2022.

[43] I. Luévanos-Soto, A. Luévanos-Rojas, V. M. Moreno-Landeros and G. Santiago-Hurtado, Minimum area for circular isolated footings with eccentric column taking into account that the surface in contact with the ground works partially in compression, *Coupled Systems Mechanics*, vol.13, no.3, pp.201-217, 2024.

[44] A. Luévanos-Rojas, B. L. Estrada-Mendoza and M. Juárez-Ramirez, Comparative study for minimum areas in contact with the ground of rectangular and circular isolated footings working partially under compression, *Boletín Ciencias de la Tierra*, vol.55, no.1, pp.85-98, 2024.

[45] P. Montes-Paramo, A. Luévanos-Rojas, S. López-Chavarría, M. Medina-Elizondo and R. Sandoval-Rivas, Optimal area for rectangular combined footings assuming that contact surface with the soil works partially to compression, *Ingeniería Investigación y Tecnología*, vol.24, no.2, pp.1-15, 2023.

[46] A. Luévanos-Rojas, New model for complete design of rectangular isolated footings taking into account that the contact surface works partially in compression, *Revista ALCONPAT*, vol.10, no.3, pp.192-219, 2023.

[47] D. S. Kim-Sanchez, A. Luévanos-Rojas, J. D. Barquero-Cabrero, S. López-Chavarría, M. Medina-Elizondo and I. Luévanos-Soto, A new model for the complete design of circular isolated footings considering that the contact surface works partially under compression, *International Journal of Innovative Computing, Information and Control*, vol.18, no.6, pp.1769-1784, 2022.

[48] I. Luévanos-Soto, A. Luévanos-Rojas, V. M. Moreno-Landeros and G. Santiago-Hurtado, Minimum cost design for circular isolated footings with eccentric column taking into account that the surface in contact with the ground works partially in compression, *Coupled Systems Mechanics*, vol.13, no.4, pp.311-335, 2024.

[49] N. M. Saleh, A. E. Alsaied and A. M. Elleboudy, Performance of skirted strip footing subjected to eccentric inclined load, *Electronic Journal of Geotechnical Engineering*, vol.13, no.1, pp.1-13, 2008.

[50] N. M. Saleh, A. M. Elleboudy and A. E. Elsaied, Behavior of skirted strip footing under eccentric load, *Proc. of the 17th International Conference on Soil Mechanics and Geotechnical Engineering*, Alexandria, Egypt, 2009.

[51] O. Farzaneh, J. Mofidi and F. Askari, Seismic bearing capacity of strip footings near cohesive slopes using lower bound limit analysis, *Proc. of the 18th International Conference on Soil Mechanics and Geotechnical Engineering*, Paris, France, 2013.

[52] E. Sadoglu, Design optimization for symmetrical gravity retaining walls, *Acta Geotechnica Slovenica*, vol.11, no.2, pp.70-79, 2014.

[53] W. Fang and L. Shi, Lower bound solution of foundation bearing capacity beneath strip footing based on parabolic mohr failure criterion, *Advances in Civil Engineering*, vol.2020, pp.1-8, https://doi.org/10.1155/2020/8897777, 2020.

[54] S. Keawsawasvong and B. Ukritchon, A practical method for the optimal design of continuous footing using ant-colony optimization, *Acta Geotechnica Slovenica*, vol.12, no.2, pp.45-55, 2016.

[55] B. Mazouz, T. Mansouri, M. Baazouzi and K. Abbeche, Assessing the effect of underground void on strip footing sitting on a reinforced sand slope with numerical modeling, *Engineering, Technology & Applied Science Research*, vol.12, no.4, pp.9005-9011, 2022.

[56] N. Yalaoui, H. Trouzine, M. Meghachou and T. Miranda, Geotextile reinforced strip footing: Numerical modeling and analysis, *Mathematical Modelling of Engineering Problems*, vol.10, no.2, pp.398-404, 2023.

[57] S. S. Pusadkar, S. S. Harne and S. W. Thakare, Performance of strip footing above multiple square voids in C-Ø soil, *International Journal of Engineering Research & Technology (IJERT)*, vol.6, no.6, pp.816-823, 2017.

[58] S. Jaiswal, A. Srivastava and V. B. Chauhan, Performance of strip footing on sand bed reinforced with multilayer geotextile with wraparound ends, *Proc. of Indian Geotechnical Conference 2020*, Andhra University, Visakhapatnam, Indian, 2020.
[59] J. C. McCormac and R. H. Brown, *Design of Reinforced Concrete*, John Wiley & Sons, Inc., Mexico City, Mexico, 2014.
[60] ACI 318-19 (American Concrete Institute), *Building Code Requirements for Structural Concrete and Commentary*, Committee 318, New York, U.S.A., 2019.

Author Biography

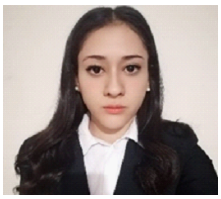

Rosa Margarita Luévanos-Soto received the Master's degree in Administration and Senior Management and the degree of Doctor in Administration and Senior Management from the Facultad de Contaduría y Administración of the Universidad Autónoma de Coahuila, México, in 2020 and 2024, respectively. She is a professor and researcher of the Facultad de Contaduría y Administración, Torreón Campus of the Universidad Autónoma de Coahuila. Her research interests are mathematical models applied to administration.

Arnulfo Luévanos-Rojas obtained his Bachelor's degree in Civil Engineering in 1981 from Facultad de Ingeniería, Ciencias y Arquitectura, Gómez Palacio Campus of the Universidad Juárez del Estado de Durango, México, his Master's degree in Science with Specialization in Structures in 1983 from Instituto Politécnico Nacional, Distrito Federal, México, his Master's degree in Science with Specialization in Planning and Construction of Works in 2000 from Facultad de Ingeniería, Ciencias y Arquitectura, Gómez Palacio Campus of the Universidad Juárez del Estadode Durango, México, his Master's degree in Administration in 2004 from Facultad de Contaduría y Administración, Torreón Campus of the Universidad Autónoma de Coahuila, México, and his Doctor degree in Engineering with Specialization in Planning Systems and Construction in 2009 from Facultad de Ingeniería, Ciencias y Arquitectura, Gómez Palacio Campus of the Universidad Juárez del Estado de Durango, México. He was a professor and researcher of the Facultad de Ingeniería, Cienciasy Arquitectura, Gómez Palacio Campus of the Universidad Juárez del Estadode Durango, México, from 2006 to 2015, and of the Facultad de Contaduría y Administración, Torreón Campus of the Universidad Autónoma de Coahuila, México since 2015 to date. He has published more than 146 papers in journals indexed in the Web of Science. His research interests are mathematical models applied to engineering and administration. He is member of the National System of Researchers of México (Level I from 2016-2022 and Level II from 2023-2027). He is an Honorary State Researcher for the State of Coahuila, México. He has received several distinctions: Distinguished Professor by ULSA (Universidad La Salle Laguna) 2002, 2007, 2010; Researcher of the year 2023 by UAC (Universidad Autónoma de Coahuila); Best scientific article of the year 2023 by UAC (Universidad Autónoma de Coahuila); He has been included in the "2023 World's Top 2% Scientists List" by Stanford University, Mathematical Engineering Excellence Award by Math Scientist Awards (2025).

Inocencio Luévanos-Soto obtained his Bachelor's degree in Architect in 2009, his Master's degree in Science with Specialization in Planning and Construction of Works in 2012, and his Doctor degree in Engineering with Specialization in Planning Systems and Construction in 2024, all from Facultad de Ingeniería, Ciencias y Arquitectura, Gómez Palacio Campus of the Universidad Juárez del Estado de Durango, México. He is a professor and researcher of the Facultad de Ingeniería, Ciencias y Arquitectura, Gómez Palacio Campus of the Universidad Juárez del Estado de Durango, since 2010 to date. His research interests are mathematical models applied to engineering and architect.